Supplementary Information

Directed Gas Phase Formation of Methylgermylene ($HGeCH_3$)

Zhenghai Yang,[a] Chao He,[a] Srinivas Doddipatla,[a] Vladislav S. Krasnoukhov,[b] Valeriy N. Azyazov,[b,c] Alexander M. Mebel,[d]* Ralf I. Kaiser [a]*

[a] *Department of Chemistry, University of Hawai'i at Manoa, Honolulu, HI 96822, USA*

[b] *Samara National Research University, Samara 443086, Russian Federation*

[c] *Lebedev Physical Institute, Samara 443011, Russian Federation*

[d] *Department of Chemistry and Biochemistry, Florida International University, Miami, Florida 33199, USA*

*Email: mebela@fiu.edu, ralfk@hawaii.edu

EXPERIMENTAL & COMPUTATIONAL

EXPERIMENTAL

The bimolecular reaction of methylidyne (CH, $X^2\Pi$) with germane (GeH_4) was performed under single collision conditions in a crossed molecular beam machine at the University of Hawaii.[1] The pulsed supersonic methylidyne beam was produced via photodissociation (COMPex 110, Coherent, Inc.; 248 nm; 30 Hz) of helium-seeded (99.9999%; AirGas) bromoform ($CHBr_3$, Sigma-Aldrich, ≥ 99 %) held in a stainless steel bubbler at 283 K at a total pressure of 2.2 atm.[2] After passing through the skimmer, the methylidyne beam was velocity selected by a four-slot chopper wheel with a peak velocity of v_p=1851 ± 11 m s^{-1} and a speed ratio S of 13.4 ± 0.6 (Table S1). Using laser-induced fluorescence, the methylidyne radical beam was characterized by a rotational temperature of 14 ± 1 K.[3] The supersonic beam of neat germane (Linde, 99.999 %) at a backing pressure of 550 Torr with a peak velocity of v_p=529 ± 5 m s^{-1} and a speed ratio S of 9.0 ± 0.7 (Table S1) crossed perpendicularly with the methylidyne beam, resulting in a collision energy of 20.6 ± 0.3 kJ mol^{-1} and a center-of mass angle Θ_{CM} of 60.5 ± 0.4°. Each supersonic beam initiated in a piezoelectric pulse valve, which was operated at a repetition rate of 60 Hz, a pulse width of 80 μs, and a peak voltage of −400 V. The secondary pulse valve was triggered 110 μs prior to the primary pulse valve, introducing the pure germane gas. The detector is housed within a triply differentially pumped chamber and rotatable in the plane defined by both reactant beams. It comprises a Brink-type ionizer,[4] a quadrupole mass spectrometer (QMS), and a Daly-type ion counter.[5] The neutral reaction products entering the detector were ionized by electron impact (80 eV), filtered based on their mass-to-charge ratios (m/z) utilizing a QMS (Extrel; QC 150) equipped with a 2.1 MHz oscillator, and eventually recorded by a Daly-type ion counter. Up to 1.3×10^6 time-of-flight (TOF) spectra were collected at laboratory angles between $0 \leq \Theta \leq 69°$ with respect to the methylidyne beam ($\Theta = 0°$). Based on user-defined center-of mass (CM) translational energy $P(E_T)$ and angular $T(\theta)$ flux distributions, a forward convolution routine was used to analyze the laboratory data. These functions, which define the reactive differential cross section $I(u, \theta) \sim P(u) \times T(\theta)$ with the center-of-mass velocity u, are varied until an acceptable fit of the laboratory frame (LAB) TOF spectra and angular distributions is obtained.[6] The error ranges of the $P(E_T)$ and $T(\theta)$ functions are determined within 1σ limits of the corresponding laboratory angular distribution while maintaining a good fit of the laboratory TOF spectra.

COMPUTATIONAL

Geometries of the reactants, products, intermediates, and transition states involved in the CH + GeH_4 reaction were optimized using the doubly hybrid DFT B2PLYPD3 method[7] with Dunning's correlation-consistent cc-pVTZ basis set[8] and vibrational frequencies and zero-point vibrational energy corrections (ZPE) were calculated at the same B2PLYPD3/cc-pVTZ level of theory. Single-point energies of the optimized structures were refined using the explicitly correlated coupled clusters CCSD(T)-F12/cc-pVQZ-f12 method,[9] which closely approximates CCSD(T)/CBS energies, i.e. the energies within the coupled clusters theory with single and double excitations with perturbative treatment of triple excitations in the complete basis set limit. The expected accuracy of the CCSD(T)-F12/cc-pVQZ-f12//B2PLYPD3/cc-pVTZ + ZPE(B2PLYPD3/cc-pVTZ) relative energies is expected to be better than within 4 kJ mol^{-1}.[10] T1 diagnostic values below 0.02 (Table S2) indicate that the single-reference approach is appropriate for the structures relevant to the primary CH + GeH_4 reaction under single-collision conditions in crossed molecular beams. The values above 0.03 are found only for two transition states for secondary isomerization reactions **p1**-**p2** (0.043) and **p4**-**p5** (0.039). These two transition states may have a moderate multireference character making their CCSD(T) energies somewhat less reliable than for the rest of the structures. However, since these transition states are not significant for the main subject of this article, we did not pursue multireference calculations here. B2PLYPD3 calculations were performed using the Gaussian 09[11] software package, whereas the CCSD(T)-F12 calculations were carried out using Molpro 2010.[12] Rice-Ramsperger-Kassel-Marcus (RRKM) theory,[13] was used to compute energy-dependent rate constants of all unimolecular reaction steps on the $CGeH_5$ PES ensuing the initial insertion of the CH radical into a Ge-H bond forming **i1**. Internal energy dependent rate constants were computed within the harmonic approximation using B2PLYPD3/cc-pVTZ frequencies using our in-house code,[14] which automatically processes GAUSSIAN 09 log files to assess numbers of states for transition states and densities of states for local minima employing the direct count method. The internal energy was assumed to be equal to the sum of the collision energy and the chemical activation energy, that is, negative of the relative energy of a species with respect to the reactants. Only one energy level was considered throughout as at a zero-pressure limit corresponding to crossed molecular beams conditions. For the H loss channels forming **p1** and **p3** without exit barriers, rate constants were computed using microcanonical variational

transition state theory (VTST).[13, 15] To find the minimal value of the H elimination rate constant $k(E)$ for a particular channel, we scanned the minimal potential energy profile (MEP) along the breaking Ge-H or C-H bond. To obtain the MEP structures, we carried partial B2PLYPD3/cc-pVTZ geometry optimization with fixed values of the Ge-H or C-H distance with all other geometric parameters being optimized. Then, we computed 3N-7 vibrational frequencies projecting the reaction coordinate out and refined single-point energies along the MEP at the CCSD(T)-F12/cc-pVQZ-f12 level. RRKM and VTST rate constants were utilized to compute product branching ratios by solving first-order kinetic equations within steady-state approximation.[14-15]

Table S1: Peak Velocity (v_p) and Speed Ratios (S) of the Methylidyne (CH) and Germane (GeH_4) Beams along with the Corresponding Collision Energy (E_C) and Center-of-Mass Angle Θ_{CM}.

beam	v_p (m s^{-1})	S	E_c (kJ mol^{-1})	Θ_{CM} (deg)
CH	1851 ± 11	13.4 ± 0.6		
GeH_4	529 ± 5	9.0 ± 0.7	20.6 ± 0.3	60.5 ± 0.4

Table S2: Cartesian coordinates (Å) and frequencies (cm^{-1}) of reactants, intermediates, transition states, and products. Point groups and ground electronic wave functions are also included. Total energies for each species calculated at the B2PLYPD3/cc-pVTZ and CCSD(T)-F12/cc-pVQZ-f12 levels of theory are given in hartree.

Reactants

GeH_4, T_d, $^1A_1$

Ge	0.000000	0.000017	0.000000
H	1.246688	0.880010	0.000000
H	-1.245291	0.881987	0.000000
H	-0.000699	-0.881278	1.245807
H	-0.000699	-0.881278	-1.245807

Frequencies

844.05	844.40	844.50
945.58	945.97	2194.31
2199.85	2199.97	2200.01

Total energy
B2PLYPD3: -2079.035423
CCSD(T)-F12: -2077.902806

T1 diagnostic: 0.01082859

CH, $C_{\infty v}$, $^2\Pi$

C	0.000000	0.000000	0.159796
H	0.000000	0.000000	-0.958776

Frequencies
2874.29

Total energy
B2PLYPD3: -38.457259
CCSD(T)-F12: -38.421103

T1 diagnostic: 0.00892159

Products

p1 (singlet), C_s, $^1A'$

Ge	-0.451118	-0.052028	-0.000001
C	1.542425	0.001672	-0.000007
H	-0.588058	1.532333	0.000001
H	1.890426	0.555865	-0.874791

H	1.988528	-0.988951	-0.000116
H	1.890344	0.555613	0.874976

Frequencies

141.19	548.61	574.46
613.01	899.43	1242.66
1449.80	1462.83	1929.93
3030.12	3096.23	3148.40

Total energy
B2PLYPD3: -2117.096747
CCSD(T)-F12: -2115.925884

T1 diagnostic: 0.01217545

p1 (triplet), C_s, ^3A”

Ge	-0.429486	-0.055332	0.000000
C	1.547326	0.053321	0.000004
H	-1.259331	1.244199	0.000006
H	1.879488	0.578286	0.892344
H	1.879373	0.579330	-0.891768
H	1.960080	-0.951129	-0.000619

Frequencies

93.72	526.79	561.09
792.21	855.31	1243.05
1463.42	1467.71	2078.39
3062.29	3152.39	3165.75

Total energy
B2PLYPD3: -2117.054057
CCSD(T)-F12: -2115.909596

T1 diagnostic: 0.01509835

p2, C_{2v}, $^1A_1$

Ge	0.9543659028	-0.0128866046	0.3569928667
C	-0.822730395	-0.0133526264	0.3547112737
H	1.7693048439	1.109663032	-0.2585404627
H	1.7680168916	-1.1352151585	0.9746475231
H	-1.3835336079	0.7939320221	-0.0895599389
H	-1.3840916354	-0.8210146646	0.7975977381

Frequencies

368.38	461.36	727.31
749.59	818.29	839.21

880.71	1399.73	2220.17
2233.55	3175.42	3279.82

Total energy
B2PLYPD3: -2117.077188
CCSD(T)-F12: -2115.906298

T1 diagnostic: 0.01455646

p3 (triplet), C_s, ^3A”

Ge	-0.013881	-0.301732	0.000000
C	-0.013881	1.601102	0.000000
H	-1.461453	-0.786061	0.000000
H	0.700025	-0.830220	1.248282
H	0.700025	-0.830220	-1.248282
H	0.588894	2.495303	0.000000

Frequencies

121.32	474.87	582.75
628.55	680.66	868.02
894.05	897.31	2165.75
2168.54	2197.46	3248.81

Total energy
B2PLYPD3: -2116.989148
CCSD(T)-F12: -2115.817373

T1 diagnostic: 0.01479238

p3 (singlet), C_1, ^1A

Ge	-0.0174942195	-0.303328902	-0.0551353534
C	0.0325175983	1.6309521411	0.2618486634
H	-1.4521690178	-0.8215603481	-0.0562003702
H	0.6749467285	-0.7323662964	1.2524611693
H	0.7524308141	-0.8923080073	-1.2445016565
H	0.9863480965	1.9968684128	-0.1584724525

Frequencies

274.76	336.95	540.83
615.90	805.87	855.15
892.02	909.96	2128.73
2151.73	2203.78	2991.79

Total energy
B2PLYPD3: -2116.960854
CCSD(T)-F12: -2115.792208

T1 diagnostic: 0.01592200

p4, C_s, ^2A”

Ge	0.466051	0.000002	0.001537
C	-1.529362	0.000019	0.011246
H	-1.959779	0.891924	0.464641
H	-1.959633	-0.891426	0.465704
H	-1.818044	-0.000683	-1.046995

Frequencies

513.02	562.87	591.38
1234.86	1374.46	1457.62
3008.29	3090.47	3122.79

Total energy
B2PLYPD3: -2116.482223
CCSD(T)-F12: -2115.308590

T1 diagnostic: 0.01168978

p5, C_1, ^2A

Ge	0.39163	-0.05335	0.01324
C	-1.50577	0.03363	-0.04143
H	0.67608	1.46046	-0.33789
H	-2.13287	-0.8315	-0.2235
H	-2.04073	0.87642	0.38634

Frequencies

425.94	557.18	562.17
690.84	826.06	1402.11
1955.32	3115.29	3212.97

Total energy
B2PLYPD3: -2116.436078
CCSD(T)-F12: -2115.264358

T1 diagnostic: 0.02955436

p6, C_s, ^2A’

Ge	-0.9584313578	0.2966049932	0.6414931035
C	0.7755113369	0.4512556933	0.6413319664

H -1.6822201457 -1.0422979794 0.6410874037
H -1.8456946628 1.5240909268 0.642022679
H 1.7682248294 0.0441553662 0.6410848474

Frequencies

230.32	399.31	571.97
686.90	858.22	961.68
2191.49	2234.94	3317.82

Total energy
B2PLYPD3: -2116.389604
CCSD(T)-F12: -2115.218019

T1 diagnostic: 0.01816002

p7, C_s, ^2A”
Ge -0.006179 0.255302 0.0
C -0.006179 -1.737927 0.0
H 1.506081 0.525013 0.0
H -0.635635 0.866445 1.253459
H -0.635635 0.866445 -1.253459

Frequencies

324.12	407.98	591.67
799.22	864.58	892.61
2147.53	2172.99	2173.03

Total energy
B2PLYPD3: -2116.311036
CCSD(T)-F12: -2115.134312

T1 diagnostic: 0.01684392

Intermediates

i1, C_s, ^2A’
Ge -0.8633631714 -0.3269947201 -0.0317862896
C 0.9636065532 0.2696007839 -0.0303753288
H -1.80512638 0.8744789655 -0.1271196279
H -1.1594743546 -1.1076835762 1.2499428828
H -1.1392004303 -1.2482403117 -1.2271462955
H 1.2721313791 1.1709708091 -0.5391517193
H 1.7501674041 -0.2966569505 0.4463433783

Frequencies

24.85	484.18	502.98
602.46	652.71	809.07
866.53	899.86	912.68
1407.31	2155.46	2184.56
2187.58	3160.13	3264.78

Total energy
B2PLYPD3: -2117.664787
CCSD(T)-F12: -2116.494091

T1 diagnostic: 0.01132306

i2, C_s, $^2A'$

Ge	0.816074148	-0.0195047819	-0.5237982848
C	-1.1270937182	-6.901092E-4	-0.2383439732
H	1.4751935584	1.2486514058	0.0444834949
H	1.4604883825	-1.2631239186	0.1115904289
H	-1.3398421855	0.0290772927	0.8297552545
H	-1.5686987356	0.8741264501	-0.7080634214
H	-1.5787794497	-0.8942913389	-0.6607484989

Frequencies

152.35	502.84	543.78
592.51	822.46	870.21
871.93	1272.41	1470.04
1475.99	2119.68	2146.96
3058.71	3140.90	3161.04

Total energy
B2PLYPD3: -2117.695359
CCSD(T)-F12: -2116.526156

T1 diagnostic: 0.01269505

Transition states

i1-i2, C_s, $^2A'$

Ge	0.9366948649	-0.0529780116	-0.5158462117
C	-0.9840412728	-0.0459171919	-0.4387299992
H	1.5565128499	1.2688698321	-0.9504252642
H	1.5399183326	-1.309798514	-1.1296649837
H	0.0097772814	-0.1396985114	0.8177442678
H	-1.5211223416	0.8688137329	-0.235918659
H	-1.5339467144	-0.972415336	-0.36445715

Frequencies

1773.17*i*	343.38	502.11
522.27	610.14	673.92
791.57	832.51	971.23
1372.89	1837.29	2166.58
2203.24	3158.47	3273.99

Total energy
B2PLYPD3: -2117.604976
CCSD(T)-F12: -2116.434698

T1 diagnostic: 0.02149244

i1-p2, C_s, $^2A'$

Ge	0.7553575414	-0.0132217986	-0.6386860482
C	-0.9935197798	-0.0131211962	-0.4136643462
H	1.5738543871	1.2641519111	-0.7129592753
H	1.5651401108	-1.2905432133	-0.7795358065
H	2.2116438966	-0.0915652453	2.1742588855
H	-1.5474221613	0.9075244616	-0.317031174
H	-1.5537009948	-0.9337539194	-0.3650162352

Frequencies

201.06*i*	42.84	86.89
452.48	465.80	760.32
782.83	821.86	878.05
946.44	1408.81	2223.66
2235.37	3177.35	3280.08

Total energy
B2PLYPD3: -2117.575881
CCSD(T)-F12: -2116.406481

T1 diagnostic: 0.01514421

i1-p6, C_s, $^2A'$

Ge	0.309579	-0.067126	0.
C	-1.593036	0.016214	0.
H	1.225176	-0.120272	-1.244415
H	1.225227	-0.12007	1.244386
H	-2.172186	-0.907842	0.
H	0.115991	1.76782	0.
H	-0.742516	1.431116	0.

Frequencies

1543.05*i*	161.90	361.65
565.69	580.05	708.16
846.20	874.19	904.38
1053.96	1631.55	2008.98
2087.17	2089.55	3114.22

Total energy
B2PLYPD3: -2117.502349
CCSD(T)-F12: -2116.332801

T1 diagnostic: 0.01506166

i1-p7, C_1, ^2A

Ge	-0.37286	0.02704	-0.00295
C	1.52514	-0.57065	0.04517
H	-1.02889	-0.11829	1.37193
H	-1.17671	-0.75534	-1.04389
H	-0.31358	1.50549	-0.39634
H	2.79855	0.62639	-0.39862
H	2.50145	1.30047	0.2902

Frequencies

1026.72*i*	88.49	427.46
469.44	510.43	628.02
817.11	878.53	899.32
1307.89	1431.17	1715.05
2162.07	2169.02	2175.32

Total energy
B2PLYPD3: -2117.460245
CCSD(T)-F12: -2116.291253

T1 diagnostic: 0.01798176

i2-p2, C_s, $^2A'$

Ge	0.7583190946	-0.0042727747	0.0746727895
C	-1.0104821111	-0.0232513834	-0.005297088
H	1.5278275648	1.0301389549	0.8761460099
H	1.62050139	-0.9890677928	-0.6942920746
H	-1.6049720354	0.6783500636	0.5581717844
H	-1.4228046951	1.3984066677	-1.8548298366
H	-1.5382992077	-0.7741067353	-0.5716815846

Frequencies

395.10*i*	167.54	180.10

451.51	466.97	761.37
789.74	824.86	875.13
909.50	1405.26	2227.30
2241.42	3179.70	3284.39

Total energy
B2PLYPD3: -2117.576294
CCSD(T)-F12: -2116.405715

T1 diagnostic: 0.01604875

i2-p5, C_1, ^2A

Ge	0.39084	-0.00287	-0.01243
C	-1.47061	-0.22666	-0.04029
H	1.38835	-1.16151	0.35895
H	-1.93177	0.08744	0.8877
H	-1.80712	-1.20043	-0.39079
H	-0.44246	2.15626	0.2626
H	-0.89039	1.56997	-0.47897

Frequencies

1380.74*i*	131.68	329.85
339.38	531.39	578.61
705.14	767.46	1132.34
1349.46	1432.55	1519.30
1887.24	3089.17	3218.45

Total energy
B2PLYPD3: -2117.519860
CCSD(T)-F12: -2116.355840

T1 diagnostic: 0.02837445

p1-p2, C_1, ^1A

Ge	-0.397133	-0.033690	-0.039991
C	1.483386	0.071063	-0.041034
H	-0.728497	1.391884	0.495598
H	2.033431	-0.853929	-0.180712
H	0.375924	-0.826754	1.136626
H	2.127079	0.940519	0.074387

Frequencies

1088.74i	542.31	693.50
741.05	846.73	933.69

980.07	1432.07	1833.29
2045.69	3098.31	3199.68

Total energy
B2PLYPD3: -2117.022792
CCSD(T)-F12: -2115.850756

T1 diagnostic: 0.04305191

p2-p6, C_s, $^2A'$

Ge	0.388579	-0.030461	-0.000001
C	-1.311671	0.392895	0.000011
H	0.819562	-1.483548	0.000025
H	1.522032	0.985343	-0.000009
H	-1.894426	1.299003	-0.000020
H	-2.230452	-0.771136	0.000032
H	-2.781229	-1.412280	-0.000048

Frequencies

1016.42i	223.11	234.90
401.07	528.37	698.72
769.88	798.95	863.19
926.98	1045.74	2198.56
2237.55	2258.45	3260.00

Total energy
B2PLYPD3: -2117.550857
CCSD(T)-F12: -2116.379735

T1 diagnostic: 0.02085125

p4-p5, C_1, ^2A

Ge	-0.422089	0.021190	-0.009873
C	1.476745	0.072466	-0.039798
H	0.490555	-1.225545	0.592629
H	2.085310	0.814557	0.477222
H	2.070518	-0.701892	-0.515132

Frequencies

1275.22i	587.81	651.41
871.96	993.69	1401.70
1687.80	3074.19	3176.10

Total energy
B2PLYPD3: -2116.414492

CCSD(T)-F12: -2115.238466

T1 diagnostic: 0.03867904

Table S3: Charge distribution calculated using natural bond population analysis.

a) $GeHCH_3$ singlet

Atom	No	Charge
Ge	1	0.75894
C	2	-1.08937
H	3	-0.30038
H	4	0.21587
H	5	0.19907
H	6	0.21587

b) $GeHCH_3$ triplet

Atom	No	Charge
Ge	1	0.52664
C	2	-0.98469
H	3	-0.18195
H	4	0.21258
H	5	0.21259

c) $CHCH_3$ singlet:

Atom	No	Charge
C	1	0.03610
C	2	-0.71944
H	3	0.04967
H	4	0.18546
H	5	0.22410
H	6	0.22410

d) $CHCH_3$ triplet:

Atom	No	Charge
C	1	-0.00573
C	2	-0.70342
H	3	0.10851
H	4	0.20567
H	5	0.19748
H	6	0.19748

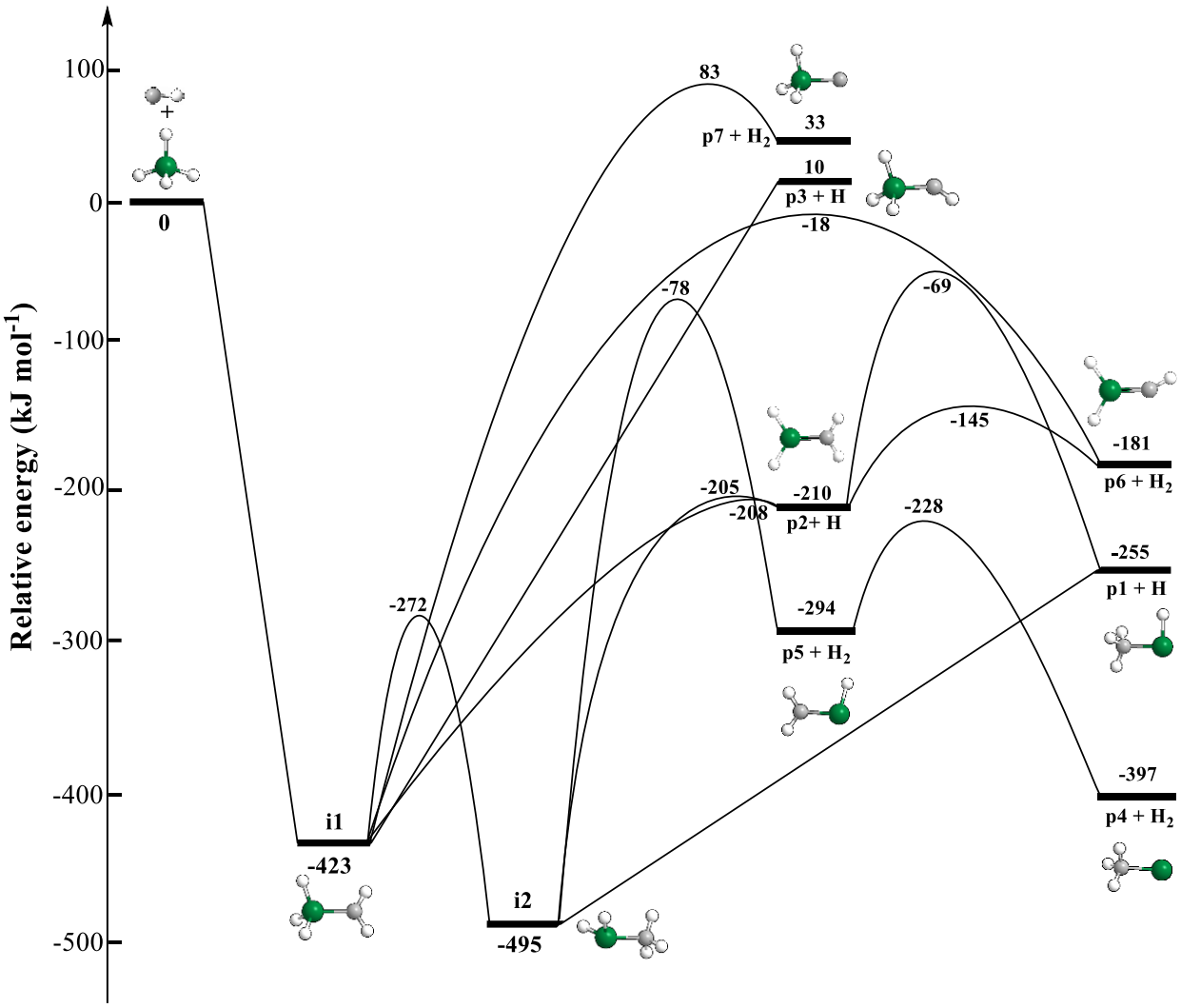

Figure S1. Potential energy surface for the reaction of the methylidyne radical with germane involving atomic and molecular hydrogen loss pathways. Optimized Cartesian coordinates of the atoms and vibrational frequencies are compiled in Table S2. Carbon, germanium, and hydrogen are color coded in gray, green, and white, respectively.

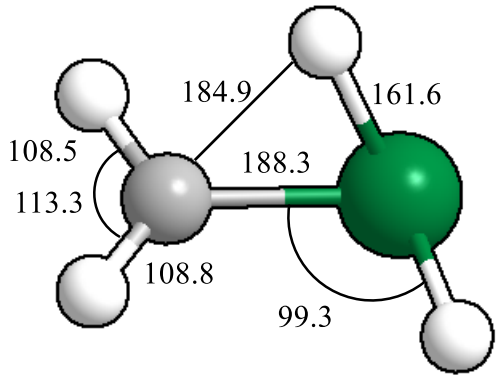

Figure S2. Molecular structure, selected bond distances (pm), and selected bond angles (degrees) of the transition state involved in the interconversion of **p1** and **p2**. Optimized Cartesian coordinates of the atoms and vibrational frequencies are presented in Table S2.

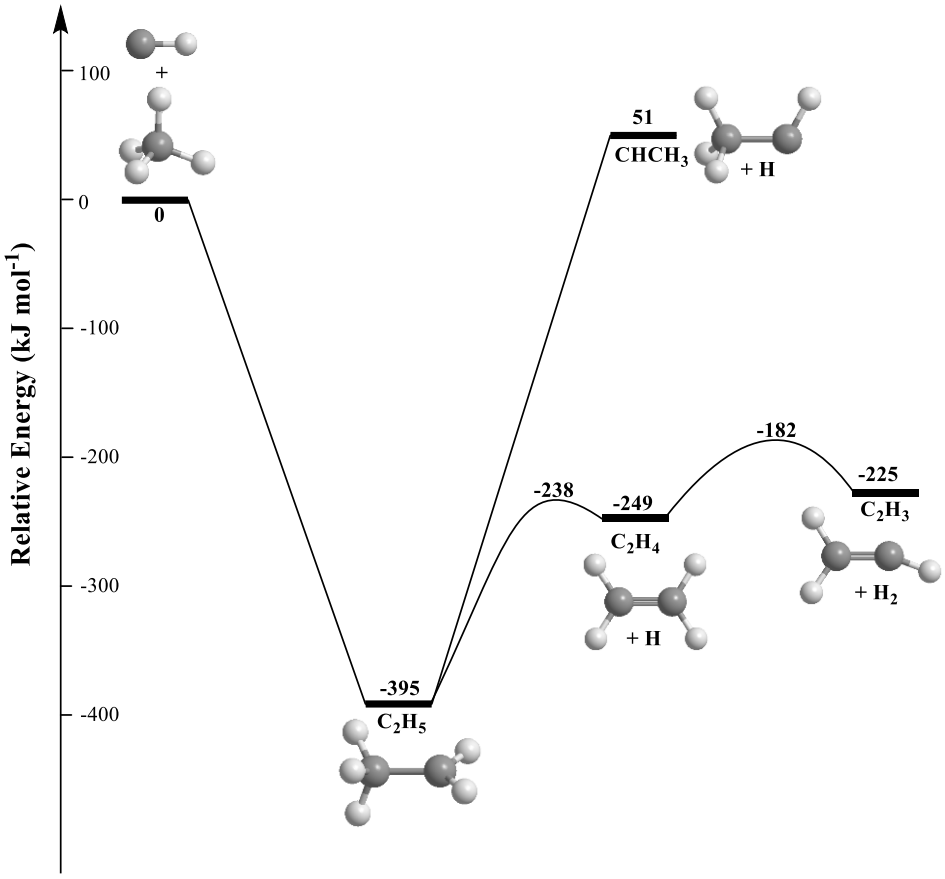

Figure S3. The potential energy surface for the reaction of the methylidyne radical with methane involving atomic and molecular hydrogen loss pathways extracted from literature.[16] Carbon and hydrogen are color coded in gray and white, respectively.

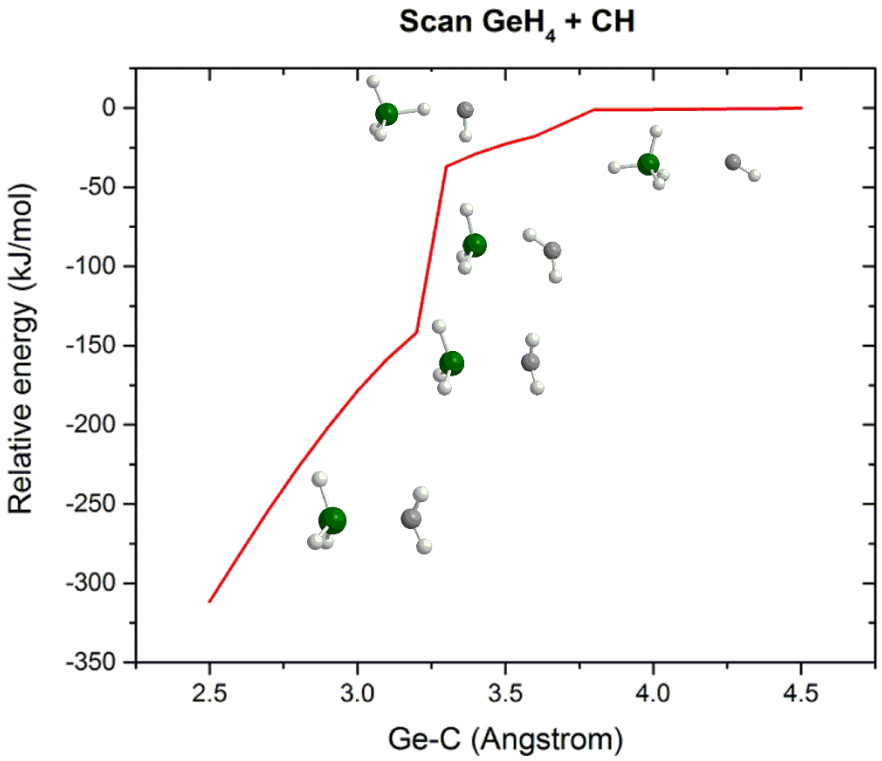

Figure S4. Calculated potential energy profile for the entrance reaction channel – CH insertion into a Ge-H bond in GeH_4 to form **i1**. Relative energies are given with respect to the CH + GeH_4 reactants. Note that the potential energy does not change smoothly because the reaction coordinate is more complex than the R(Ge-C) distance. Initially, at R > 3.8 Å, CH simply approaches GeH_4. Next, the GeH_4 rotates to point one of its H atoms toward the carbon atom and this H atom transfers from Ge to C. The H shift completes between R = 3.2 and 3.1 Å resulting in a sharp potential energy decrease. Finally, the newly formed CH_2 group approaches GeH_3 thus finalizing the formation of the Ge-C bond.

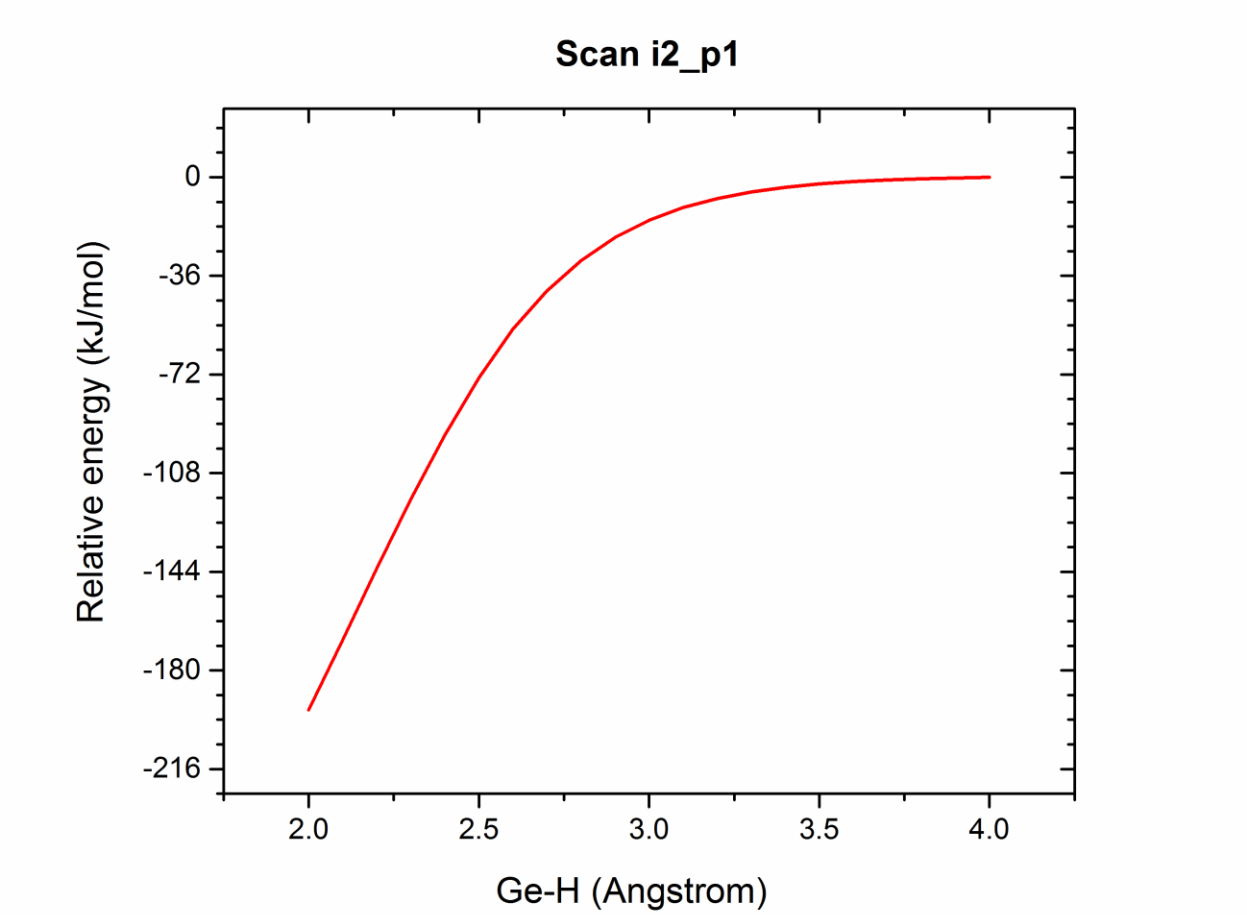

Figure S5. Calculated potential energy profile for the H loss from **i2** forming **p1** without an exit barrier. Relative energies are shown with respect to **p1** + H.

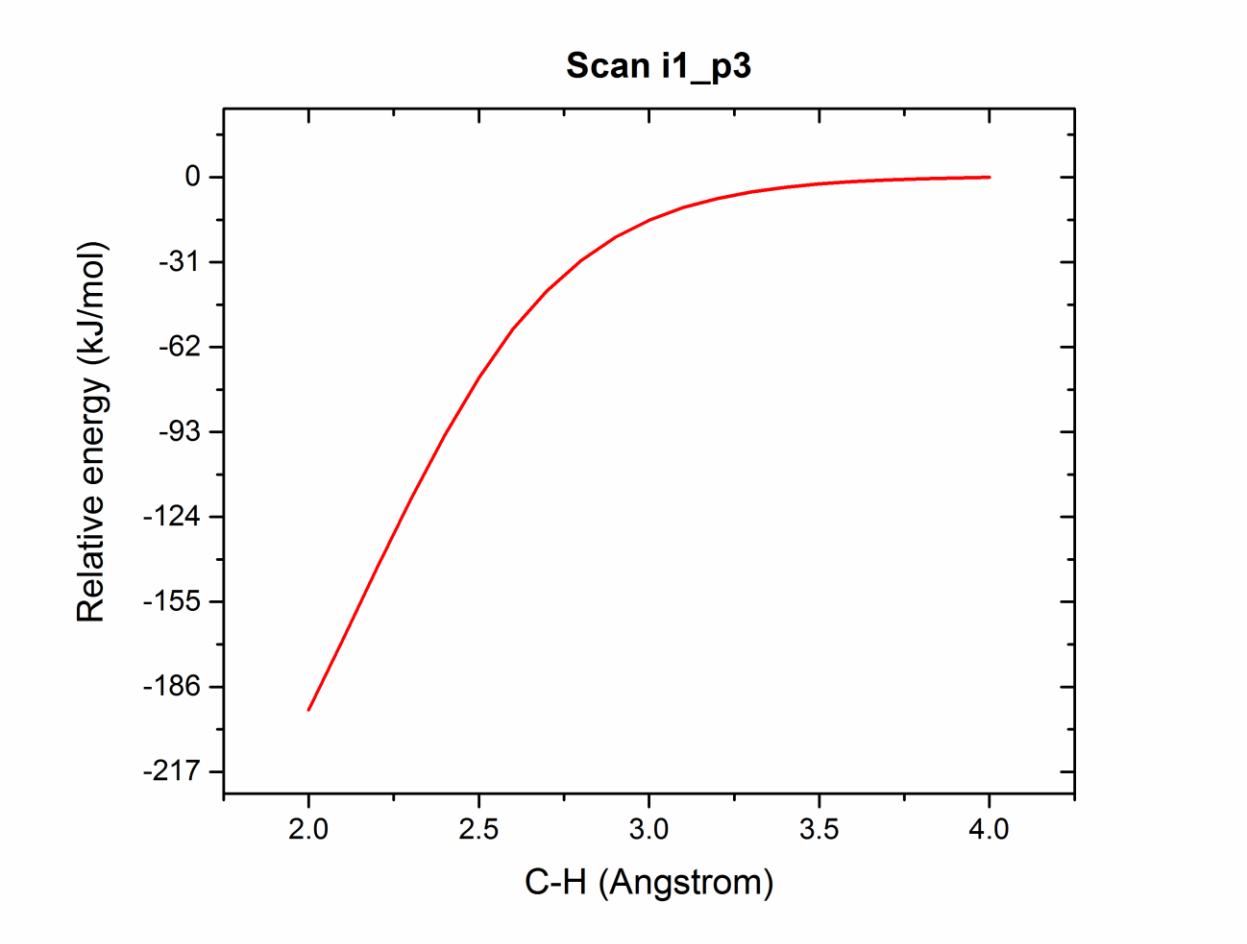

Figure S6. Calculated potential energy profile for the H loss from **i1** forming **p3** without an exit barrier. Relative energies are shown with respect to **p3** + H.

Supplementary References:

[1] a) R. I. Kaiser, P. Maksyutenko, C. Ennis, F. Zhang, X. Gu, S. P. Krishtal, A. M. Mebel, O. Kostko, M. Ahmed, *Faraday Discuss.* **2010**, *147*, 429-478; b) X. Gu, Y. Guo, F. Zhang, A. M. Mebel, R. I. Kaiser, *Faraday Discuss.* **2006**, *133*, 245-275.

[2] a) C. He, A. M. Thomas, G. R. Galimova, A. M. Mebel, R. I. Kaiser, *J. Phys. Chem. A* **2019**, *123*, 10543-10555; b) C. He, A. M. Thomas, G. R. Galimova, A. N. Morozov, A. M. Mebel, R. I. Kaiser, *J. Am. Chem. Soc.* **2020**, *142*, 3205-3213; c) A. M. Thomas, L. Zhao, C. He, G. R. Galimova, A. M. Mebel, R. I. Kaiser, *Angew. Chem. Int. Ed.* **2019**, *58*, 15488-15495.

[3] a) R. I. Kaiser, X. Gu, F. Zhang, P. Maksyutenko, *Phys.Chem.Chem.Phys.* **2012**, *14*, 575-588; b) P. Maksyutenko, F. Zhang, X. Gu, R. I. Kaiser, *Phys.Chem.Chem.Phys.* **2011**, *13*, 240-252.

[4] G. O. Brink, *Rev. Sci. lnstrum.* **1966**, *37*, 857-860.

[5] N. Daly, *Rev. Sci. lnstrum.* **1960**, *31*, 264-267.

[6] a) J. D. Bittner, Massachusetts Institute of Technology **1981**; b) P. Weiss, Lawrence Berkeley Lab., CA (USA) **1986**; c) R. I. Kaiser, T. N. Le, T. L. Nguyen, A. M. Mebel, N. Balucani, Y. T. Lee, F. Stahl, P. v. R. Schleyer, H. F. Schaefer III, *Faraday Discuss.* **2002**, *119*, 51-66.

[7] a) S. Grimme, *J. Chem. Phys.* **2006**, *124*, 034108; b) L. Goerigk, S. Grimme, *J. Chem. Theory Comput.* **2011**, *7*, 291-309; c) S. Grimme, S. Ehrlich, L. Goerigk, *J. Comput. Chem.* **2011**, *32*, 1456-1465.

[8] T. H. Dunning Jr, *J. Chem. Phys.* **1989**, *90*, 1007-1023.

[9] a) T. B. Adler, G. Knizia, H.-J. Werner, *J. Chem. Phys.* **2007**, *127*, 221106; b) G. Knizia, T. B. Adler, H.-J. Werner, *J. Chem. Phys.* **2009**, *130*, 054104.

[10] J. Zhang, E. F. Valeev, *J. Chem. Theory Comput.* **2012**, *8*, 3175-3186.

[11] M. Frisch, G. Trucks, H. Schlegel, G. Scuseria, M. Robb, J. Cheeseman, G. Scalmani, V. Barone, B. Mennucci, *Gaussian 09 Revision D. 01*, Gaussian, Inc.: Wallingford CT, **2009**.

[12] H.-J. Werner, P. Knowles, R. Lindh, F. Manby, M. Schütz, P. Celani, T. Korona, A. Mitrushenkov, G. Rauhut, *MOLPRO, version 2010.1, a package of ab initio programs*, University of Cardiff, Cardiff, UK, **2010**.

[13] a) P. J. Robinson, K. A. Holbrook, *Unimolecular reactions*, Wiley, New York, **1972**; b) H. Eyring, S. H. Lin, S. M. Lin, *Basic chemical kinetics*, John Wiley & Sons, New York, **1980**; c) J. I. Steinfeld, J. S. Francisco, W. L. Hase, *Chemical kinetics and dynamics*, *Vol. 3*, Prentice Hall, Englewood Cliffs, **1982**.

[14] C. He, L. Zhao, A. M. Thomas, A. N. Morozov, A. M. Mebel, R. I. Kaiser, *J. Phys. Chem. A* **2019**, *123*, 5446-5462.

[15] V. Kislov, T. L. Nguyen, A. Mebel, S. Lin, S. Smith, *J. Chem. Phys.* **2004**, *120*, 7008-7017.

[16] a) https://atct.anl.gov/Thermochemical%20Data/version%201.122g/index.php; b) A. M. Mebel, K. Morokuma, M.-C. Lin, *J. Chem. Phys.* **1995**, *103*, 3440-3449.